



Robust Ramsey interferometer based on a single Rydberg polariton

JIABEI FAN,¹ YUECHUN JIAO,^{1,2,*}  CHANGCHENG LI,¹
JINGXU BAI,¹ JIANMING ZHAO,^{1,2,3}  AND SUOTANG JIA^{1,2}

¹State Key Laboratory of Quantum Optics and Quantum Optics Devices, Institute of Laser Spectroscopy, Shanxi University, Taiyuan 030006, China

²Collaborative Innovation Center of Extreme Optics, Shanxi University, Taiyuan 030006, China

³zhaojm@sxu.edu.cn

*ycjiao@sxu.edu.cn

Abstract: We demonstrate a robust single-photon Ramsey interferometer based on a single Rydberg excitation, where the photon is stored as a Rydberg polariton in an ensemble of atoms. This coherent conversion of the photon to Rydberg polariton enables to split an incoming photon into a superposition state of two Rydberg states by applying microwave fields, which constructs two paths of interferometer. Ramsey interference fringes are demonstrated when we scan either the detuning of the microwave or the free evolution time, from which we can obtain the resonant transition frequency of two Rydberg states. We use the Ramsey-like sequence to demonstrate coherent manipulation of the stored single-photon to construct different interference patterns. In addition, the robustness of the Ramsey interferometer to the fluctuation of incoming photon numbers and optical depth (OD) of the atomic ensemble is tested, showing that the coherent of Ramsey interferometer is preserved for input photon number in a range of $R_{in} < 15$ and for OD varying from 1.0 to 4.0. The robust interferometer will find its applications in quantum precision measurement.

© 2023 Optica Publishing Group under the terms of the [Optica Open Access Publishing Agreement](#)

1. Introduction

Interferometric measurements offer extreme sensitivity and have a wide range of applications from defining time and frequency standards [1] to gravitational wave detection [2,3]. Interferometers are used to measure the phase difference between waves following different paths. An optical interferometer's sensitivity typically increases proportionately to the time that photons are maintained in a superposition of two paths. The effective time can be increased by increasing the path length or reducing the speed of light using the slow-light medium in one or both paths [4]. Interferometers rely only on the general wave properties of superposition and interference, so they are not limited to using light waves. Replacing photons with massive particles creates an interferometer [5] that has been used to measure acceleration and gravity gradient as it is sensitivity to inertial forces [6,7]. In particle interferometers where the paths are quantum states, phase information is accumulated as long as the superposition can be maintained, which can be increased by reducing the particle speed, e.g. cold trapped atoms [8,9] or stored light [10]. Precision interferometer in ultracold atomic systems, where involving trapped neutral atoms or ions, has enabled the most precise measurements ever made, which offer great potential for searches for physics beyond the standard model [11], exploring complex quantum systems [12] and realizing quantum sensors [13].

Ramsey interferometers typically involve two states of atoms that interact very weakly with external fields, which limits the sensitivity of field measurements. An interferometer involving Rydberg states has great potential for the detection of electric fields because Rydberg atoms with large DC polarizabilities and microwave transition dipole moments [14] make these atoms extremely sensitive to DC and AC electric fields [15–17], several applications including measuring

small, static electric fields with high sensitivity [18], sensing microwave fields [19], and exploiting the state-dependent forces exerted by inhomogeneous electric fields [20]. In recent years, an interferometer based on collectively single Rydberg excitation is demonstrated [19]. Not like single atoms as individual probes [21–23], collectively excitation Rydberg Ramsey interferometer is robust to the decoherence induced by external perturbations [24]. The own properties of a collectively single Rydberg Ramsey interferometer, such as the dependence of the coherent of the Rydberg Ramsey interferometer on the input photon numbers and the atomic density, are not investigated yet.

Here, we demonstrate a single-photon stored Ramsey interferometer based on a single Rydberg excitation in an ensemble of atoms. The experimental protocol is the same as the Refs. [19,24]. A photon is stored as a Rydberg polariton using electromagnetically induced transparency (EIT). The Ramsey interferometer is performed upon the stored photon by applying microwave pulses to couple two Rydberg states, $|r\rangle = |60S_{1/2}\rangle$ and $|r'\rangle = |59P_{3/2}\rangle$. We obtain the resonant transition frequency of two Rydberg states using the interferometer by scanning the free evolution time. A Ramsey-like sequence is used to demonstrate coherent manipulation of the stored photon to construct different interference patterns. Finally, we measure the visibility of the interferometer as a function of incoming photons and OD of the atomic ensemble, showing that the visibility of the Ramsey interferometer almost keeps constant for the incoming photons $R_{in} < 15$, as well it almost keeps constant at the OD range from 1.0 to 4.0 with incoming photons $R_{in} = 3$. The collectively single Rydberg excitation interferometer shows robustness against the fluctuation of incoming photon numbers and OD of the atomic ensemble over a wide range of fluctuations.

2. Experimental setup

A schematic of the experimental apparatus and the relevant atomic levels are shown in Fig. 1(a) and (b). We initially trap an ensemble of ^{133}Cs atoms in a magneto-optical trap (MOT). Subsequently, a compressed MOT and molasses are applied to increase the atomic density and decrease the atomic temperature. Then, we transfer the atoms to a cross dipole trap composed of two 1064 nm lasers with a waist of $\omega_1 = 4.3 \mu\text{m}$ and $\omega_2 = 8.0 \mu\text{m}$. The measured atomic temperature is below 40 μK using time of flight imaging and an estimated atomic cloud size with a spatial extent $4 \times 4 \times 16 \mu\text{m}^3$. The atom number and cloud density are estimated at an order of 10^3 and 10^{12}cm^{-3} by the signal absorption, respectively. The trapped atoms are initially optically pumped to the sublevel of $|g\rangle = |6S_{1/2}, F = 4, m_F = 4\rangle$ in the presence of a weak magnetic field along the quantization axis, which is defined by the propagation direction of the probe laser beam. A Rydberg EIT is utilized to store a single photon in a collective excitation Rydberg states. In the Rydberg EIT configuration, a probe laser (852 nm) with a waist of $\omega_p = 2.5 \mu\text{m}$ is resonant with the transition of $|g\rangle = |6S_{1/2}, F = 4, m_F = 4\rangle \rightarrow |e\rangle = |6P_{3/2}, F' = 5, m_{F'} = 5\rangle$, and a coupling laser (509 nm) with a beam waist of $\omega_c = 8.5 \mu\text{m}$ drives the Rydberg transition of $|e\rangle = |6P_{3/2}, F' = 5, m_{F'} = 5\rangle \rightarrow |r\rangle = |60S_{1/2}\rangle$. The probe and coupling lasers with the opposite circular polarization are counter-propagated and focused into the atomic ensemble by employing a focusing lens pair. The frequencies of probe and coupling lasers are locked to a cavity with a finesse of 150000. The timing sequence of experiments is shown in Fig. 1(c). The probe laser is turned on for 600 ns. Before the probe is switched off, we ramp down the coupling laser to zero, achieving the photon storage as a spin wave [25,26]. The Rabi frequency of the coupling laser is $\Omega_c = 2\pi \times 10.0 \text{ MHz}$. After the photon is stored, we create the two paths of the interferometer in coherent superpositions of $|r\rangle = |60S_{1/2}\rangle$ and $|r'\rangle = |59P_{3/2}\rangle$ by applying a $\pi/2$ microwave pulse lasting $t = 20 \text{ ns}$. After several hundreds of ns free evolution time, a second $\pi/2$ microwave pulse is applied to combine the two paths. Both microwave fields are emitted from a wave-guide antenna (Model: HD-180WAL150) with linear polarization. The population in each state depends on the phase difference between waves following the two paths. Finally, the coupling laser is switched on to read out the population in $|r\rangle = |60S_{1/2}\rangle$. The single photon

EIT and readout photon are collected with a single-mode fiber and detected by a single-photon avalanche detector (SPAD). The dipole trap beam is switched off during the performance of the experiment and turned on $3 \mu\text{s}$ to re-trap the atoms after the retrieval. For each MOT loading, we can repeat the sequence 5000 times with preserving the OD and not changing too much. We define the OD of the atomic ensemble as the logarithm of transmission signal with atoms (I) at resonant frequency and transmission signal without atoms (I_0), i.e., $\text{OD} = -\ln(I/I_0)$. The bottom of Fig. 1(c) shows a typical storage and retrieval signal for $n = 60$ Rydberg state without applying microwave fields and the inset shows the measured $g^{(2)}(0) = 0.44 \pm 0.05$ for the retrieved signal. The retrieval efficiency (the ratio between the retrieval photons and the input photons) is about $\sim 0.3\%$, which is limited by motional dephasing, Rydberg blockade, and finite ensemble OD.

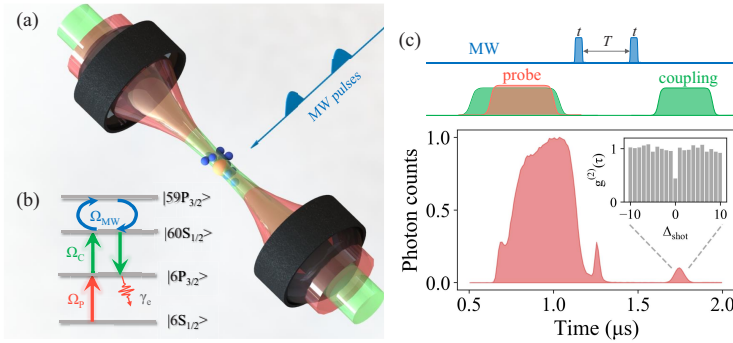


Fig. 1. (a) The schematic of the experimental apparatus. The probe and coupling lasers are counter-propagated and are focused into the atomic ensemble and recollimated by a focusing lens pair. The emitted microwave pulses are perpendicular to the lasers. (b) The energy level diagram. The probe laser (Ω_p) is resonant with the transition of $|g\rangle = |6S_{1/2}, F = 4, m_F = 4\rangle \rightarrow |e\rangle = |6P_{3/2}, F' = 5, m_{F'} = 5\rangle$, and the coupling laser (Ω_c) drives the Rydberg transition of $|e\rangle = |6P_{3/2}, F' = 5, m_{F'} = 5\rangle \rightarrow |r\rangle = |60S_{1/2}\rangle$. Microwave pulses ($\Omega_{MW}/2\pi = 12.5$ MHz) couple two adjacent Rydberg states. γ_e is the decay rate of $|6P_{3/2}\rangle$ state. (c) Timing sequence. The probe laser is turned on for 600 ns, and before the probe is switched off, we ramp down the coupling laser to zero to store a photon as a Rydberg polariton. After 570 ns of storage time, the coupling laser is switched on to read out the population in $|r\rangle = |60S_{1/2}\rangle$. The MW pulses of the Ramsey interferometer are performed between storage and retrieval. The bottom of Fig. 1(c) shows a typical storage and retrieval signal for $n = 60$ Rydberg state without applying microwave fields and the inset shows the measured $g^{(2)}(0) = 0.44 \pm 0.05$ for the retrieved signal.

3. Results and discussions

Probe photons are stored in an atomic ensemble as a collective excitation Rydberg polariton [24],

$$|\mathbf{R}\rangle = \frac{1}{\sqrt{N}} \sum_{j=1}^N e^{i(\mathbf{k}\cdot\mathbf{z}_j - \omega_r t)} |g_1 g_2 \dots r_j \dots g_N\rangle,$$

where g_j and r_j represent a atom j at the position \mathbf{z}_j in states $|g\rangle$ and $|r\rangle$ state, respectively. The phase contains both local phase terms $\mathbf{k} \cdot \mathbf{z}_j$ and a global phase, $-\omega_r t$, where ω_r is the angular frequency of the transition $|g\rangle \rightarrow |r\rangle$. The multiple Rydberg excitation is suppressed due to the Rydberg blockade mechanism, such that the retrieval photon is observed to have $g^{(2)}(0) = 0.44 \pm 0.05$ for the readout of $|r\rangle = |60S_{1/2}\rangle$, showing single photon characteristic. The purity of the single excitation strongly depends on Rydberg interaction and can be enhanced using

higher-lying Rydberg states [27,28]. The Ramsey interferometer is performed upon a single Rydberg polariton by coupling $|r\rangle$ to another collective state,

$$|R'\rangle = \frac{1}{\sqrt{N}} \sum_{j=1}^N e^{i(k \cdot z_j - \omega_{r'} t)} |g_1 g_2 \dots r'_j \dots g_N\rangle.$$

As both $|R\rangle$ and $|R'\rangle$ are collective excitation with N terms, the performance of the interferometer is independent of the number of atoms, N . This makes the interferometer robust to the fluctuation of atoms.

The probability amplitude of the interferometer is expressed as,

$$P(T, \Delta_{MW}) = 1 - \cos(\Delta_{MW} T) \quad (1)$$

where T is the free evolution time, $\Delta_{MW}/2\pi$ is the detuning of the microwave pulse relative to the resonant transition of $|r\rangle = |60S_{1/2}\rangle \rightarrow |r'\rangle = |59P_{3/2}\rangle$. The Ramsey fringes can be obtained by scanning the microwave detuning or varying the T . We first demonstrate how the detuning of microwave pulses quantitatively influences Ramsey interference fringes when we vary the free evolution time T over the range of 0-300ns. Figure 2(a) shows Ramsey interference fringes at the microwave detuning $\Delta_{MW}/2\pi = +1$ MHz (purple dot) and -10 MHz (green dot), respectively. The solid lines correspond to the fitting of the Eq. (1). It is seen that Ramsey interference fringes display a nice sinusoidal profile for the case of $\Delta_{MW}/2\pi = -10$ MHz, but there are almost no interference fringes for the case of $\Delta_{MW}/2\pi = +1$ MHz. Then, we perform a series of measurements such as in Fig. 2(a) over a detuning range of -17 MHz to 14 MHz, in steps of 1 MHz, and assemble the Ramsey interference fringes in a heat map, shown in Fig. 2(b). Each data set is taken with incoming photons $R_{in} = 3$ and normalized to its maximum value. For the case of $\Delta_{MW} = 0$, the readout signal being minimum value without any oscillation. But for the case of $\Delta_{MW} \neq 0$, the readout signal shows the sinusoidal profile, from which we can extract the oscillation frequency for each Δ_{MW} . Figure 2(c) shows the extracted oscillation frequency as a function of microwave negative detunings. Linear fittings to the data of Fig. 2(c) yield the intersection point with the x-axis, 19.415 GHz, which is the resonant frequency of $|r\rangle = |60S_{1/2}\rangle \rightarrow |r'\rangle = |59P_{3/2}\rangle$ transition. The accuracy of transmission frequency can be improved by increasing the free evolution time, which is mainly limited by motional dephasing that scrambles the information about the stored photon.

Next, we demonstrate coherent manipulation of the stored single-photon by using the Ramsey-like sequence during the storage period. We keep the two microwave pulses separation $T = 200$ ns, and change the two microwave pulses duration and further change the $\Omega_{MW} t$ with fixed $\Omega_{MW}/2\pi = 12.5$ MHz to manipulate the population of $|r\rangle = |60S_{1/2}\rangle$ Rydberg state. In Fig. 3(a), we display three interference fringes for $\Omega_{MW} t = \pi/2$, $\sqrt{2}\pi/2$, and π at $\Delta_{MW}/2\pi = 0$, respectively. The up panel of Fig. 3(a) displays a normal Ramsey interference fringe as a function of the microwave detuning $\Delta_{MW}/2\pi$ for the case of $\Omega_{MW} t = \pi/2$. Increasing both pulses' duration to $\Omega_{MW} t = \sqrt{2}\pi/2$, the fringe profile is varied, see Fig. 3(a) middle panel. Comparing with Ramsey interference fringe of $\Omega_{MW} t = \pi/2$, both fringe amplitude and contrast near the center ($\Delta_{MW}/2\pi \sim 0$) shows decrease, whereas increase at $\Delta_{MW}/2\pi \sim \pm 12.5$ MHz. This means that the microwave drives a π rotation about a Bloch vector 45° from the z-axis in a Bloch sphere and the manipulation can be used to create a Hardamard gate at $|\Delta_{MW}| = \Omega_{MW}$ [24]. In the bottom panel of Fig. 3(a), we demonstrate an interference fringe for $\Omega_{MW} t = \pi$, which means that two microwave pulses are π pulses. The first π pulse transfer initially prepared $60S_{1/2}$ state to $59P_{1/2}$ state, and the second π pulse transfer $59P_{1/2}$ state back to the $60S_{1/2}$ after some evolution time T , which means that there is no interference fringe at $\Delta_{MW}/2\pi = 0$ and deformed fringe for other Δ_{MW} . To investigate the evolution of interference fringes, we perform a series of measurements by varying the duration of both microwave pulses from 10 ns to 70 ns, corresponding to vary $\Omega_{MW} t$

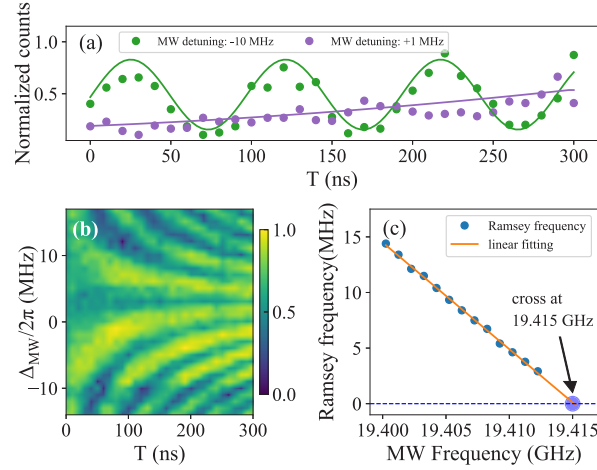


Fig. 2. (a) Ramsey interference fringes at microwave field +1 MHz detuning (purple dot) and -10 MHz detuning (green dot) with varying the free evolution time T over the range of 0-300ns. The solid lines correspond to sinusoidal fits. (b) A colormap of Ramsey interference fringes as a function of the free evolution time T and MW detuning with incoming photons $R_{in} = 3$. (c) The extracted oscillation frequency of Ramsey interference fringes (blue dots) for different microwave frequencies with negative detunings. The intersection of the linear fitting line (orange line) and the x-axis represents the resonant transition frequency of $|r\rangle = |60S_{1/2}\rangle \rightarrow |r'\rangle = |59P_{3/2}\rangle$ at 19.415GHz.

from 0.25π to 1.75π , the measured interference fringes as a function of the microwave detuning and $\Omega_{MW}t$ are displayed in Fig. 3(b), which shows that we can coherent manipulation of the stored single-photon and construct different interference patterns. We consider the interferometer as a two-level system and model the results of Fig. 3 using the master equation. Numerically solving the master equation, we obtain the interference amplitude shown as the solid lines in Fig. 3(a), which demonstrates good agreement with the experimental results.

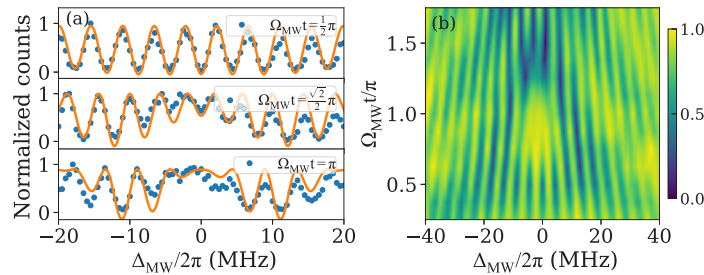


Fig. 3. (a) The Ramsey interference fringes as a function of the microwave detuning $\Delta_{MW}/2\pi$ for the case of $\Omega_{MW}t = \pi/2$ (upper), $\sqrt{2}\pi/2$ (middle), π (bottom) at $\Delta_{MW}/2\pi = 0$. The solid lines are calculated results by solving the master equation. Two microwave pulses are separated by $T=200$ ns. (b) A series of measurements with incoming photons $R_{in} = 3$ for the lasting of microwave pulse from 10 ns to 70 ns, corresponding to $\Omega_{MW}t$ from 0.25π to 1.75π .

Finally, we test the collective excited Rydberg Ramsey interferometer robustness to the fluctuation of incoming photon numbers and OD of the atomic ensemble. We first demonstrate the relation between the incoming photons and the retrieval photon numbers without microwave

sequence, shown as the blue circles in Fig. 4(a). At small incoming photon numbers ($R_{in} < 7$), the number of retrieval photons increases linearly with the incoming photons. This is because the system has the absence of interaction during storage at small incoming photons. With increasing incoming photons, the probability of storing a photon as a Rydberg polariton is increased so we can retrieve higher photons. However, the increasing number of incoming photons should eventually result in a saturation of the storage if the storage efficiency reaches the maximum, shown in the range of incoming photons $7 < R_{in} < 15$. The data is normalized to the maximum retrieval photon number. Next, we perform the interferometer to obtain the Ramsey fringes by scanning the detuning of the microwave with fixing $T=300$ ns at different incoming photons. The visibility of the Ramsey fringes is defined as the difference between the peak and minimum of the fringes divided by their sum. We extract the visibility of the fringes as a function of the incoming photons, shown as the orange squares in Fig. 4(a). The results show that the observed visibility almost keeps constant at incoming photons $R_{in} < 15$, which demonstrates the system's robustness to the fluctuation of incoming photon numbers.

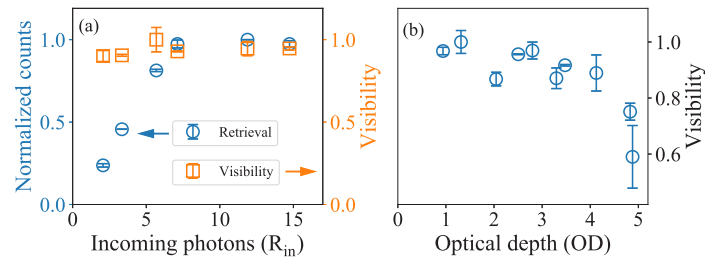


Fig. 4. (a) The normalized retrieval photons (blue circles) and visibility of the interferometer (orange squares) as a function of the incoming photons. (b) The visibility of the interferometer as a function of the OD at incoming photons $R_{in} = 3$ per shot.

Figure 4(b) shows the effect of OD on the visibility of the interferometer. The value of OD is varied by changing the power of the dipole trap, which changes the initial number of atoms. We observe that the visibility almost keeps constant when $OD < 4.0$, which shows that the coherence of the interferometer is robust to the number of atoms. At the $OD > 4.0$, the visibility rapidly reduces with increasing the OD. This could be because the strong collisions between the Rydberg polariton and ground atoms at high-density atomic ensemble cause the dephasing of Rydberg polaritons, leading to the decoherence of the interferometer. In addition, it is possible to bind the Rydberg polariton with the ground state, achieving the formation of a Rydberg molecule that also reduces visibility.

4. Conclusions

A robust Rydberg Ramsey interferometer is performed by applying microwave pulses upon a single stored photon using a collectively single Rydberg excitation. Ramsey interference fringes are obtained by scanning either the detuning of the microwave or the free evolution time, from which we get the resonant transition frequency of two Rydberg states. We also demonstrate microwave coherent manipulation of the stored photon to construct different interference patterns by using the Ramsey-like sequence. In addition, we have shown the Ramsey interferometer's robustness to the fluctuation of incoming photon numbers and OD of the atomic ensemble in a wide range by measuring the visibility of the interferometer. The robust collective excited Rydberg interferometer will be used to the quantum precision measurement.

Funding. National Natural Science Foundation of China (12120101004, 12241408, 61835007, 62175136); the Scientific Cooperation Exchanges Project of Shanxi province (202104041101015); Program for Changjiang Scholars and Innovative Research Team in University (IRT 17R70); 1331 Project of Shanxi Province.

Disclosures. The authors declare no conflicts of interest.

Data availability. Data underlying the results presented in this paper are not publicly available at this time but may be obtained from the authors upon reasonable request.

References

1. F. Riehle, "Towards a redefinition of the second based on optical atomic clocks," *C. R. Phys.* **16**(5), 506–515 (2015).
2. S. Dimopoulos, P. W. Graham, J. M. Hogan, M. A. Kasevich, and S. Rajendran, "Gravitational wave detection with atom interferometry," *Phys. Lett. B* **678**(1), 37–40 (2009).
3. B. P. Abbott, R. Abbott, and T. D. Abbott, *et al.*, "Observation of Gravitational Waves from a Binary Black Hole Merger," *Phys. Rev. Lett.* **116**(6), 061102 (2016).
4. Z. Shi, R. W. Boyd, R. M. Camacho, P. K. Vudyaasetu, and J. C. Howell, "Slow-Light Fourier Transform Interferometer," *Phys. Rev. Lett.* **99**(24), 240801 (2007).
5. C. Adams, M. Sigel, and J. Mlynek, "Atom optics," *Phys. Rep.* **240**(3), 143–210 (1994).
6. M. Kasevich and S. Chu, "Measurement of the gravitational acceleration of an atom with a light-pulse atom interferometer," *Appl. Phys. B: Photophys. Laser Chem.* **54**(5), 321–332 (1992).
7. J. B. Fixler, G. T. Foster, J. M. McGuirk, and M. A. Kasevich, "Atom Interferometer Measurement of the Newtonian Constant of Gravity," *Science* **315**(5808), 74–77 (2007).
8. T. Kovachy, P. Asenbaum, C. Overstreet, C. A. Donnelly, S. M. Dickerson, A. Sugarbaker, J. M. Hogan, and M. A. Kasevich, "Quantum superposition at the half-metre scale," *Nature* **528**(7583), 530–533 (2015).
9. B. J. Bloom, T. L. Nicholson, J. R. Williams, S. L. Campbell, M. Bishof, X. Zhang, W. Zhang, S. L. Bromley, and J. Ye, "An optical lattice clock with accuracy and stability at the 10^{-18} level," *Nature* **506**(7486), 71–75 (2014).
10. A. V. Gorshkov, A. André, M. Fleischhauer, A. S. Sørensen, and M. D. Lukin, "Universal Approach to Optimal Photon Storage in Atomic Media," *Phys. Rev. Lett.* **98**(12), 123601 (2007).
11. A. Derevianko and M. Pospelov, "Hunting for topological dark matter with atomic clocks," *Nat. Phys.* **10**(12), 933–936 (2014).
12. M. J. Martin, M. Bishof, M. D. Swallows, X. Zhang, C. Benko, J. von-Stecher, A. V. Gorshkov, A. M. Rey, and J. Ye, "A Quantum Many-Body Spin System in an Optical Lattice Clock," *Science* **341**(6146), 632–636 (2013).
13. C. L. Degen, F. Reinhard, and P. Cappellaro, "Quantum sensing," *Rev. Mod. Phys.* **89**(3), 035002 (2017).
14. T. F. Gallagher, *Rydberg Atoms* (Cambridge University Press, 1994), 1st ed.
15. H. Fan, S. Kumar, J. Sedlacek, H. Kübler, S. Karimkashi, and J. P. Shaffer, "Atom based RF electric field sensing," *J. Phys. B: At., Mol. Opt. Phys.* **48**(20), 202001 (2015).
16. J. A. Sedlacek, A. Schwettmann, H. Kübler, R. Löw, T. Pfau, and J. P. Shaffer, "Microwave electrometry with Rydberg atoms in a vapour cell using bright atomic resonances," *Nat. Phys.* **8**(11), 819–824 (2012).
17. M. Jing, Y. Hu, J. Ma, H. Zhang, L. Zhang, L. Xiao, and S. Jia, "Atomic superheterodyne receiver based on microwave-dressed Rydberg spectroscopy," *Nat. Phys.* **16**(9), 911–915 (2020).
18. A. Arias, G. Lochhead, T. M. Wintermantel, S. Helmrich, and S. Whitlock, "Realization of a Rydberg-Dressed Ramsey Interferometer and Electrometer," *Phys. Rev. Lett.* **122**(5), 053601 (2019).
19. Y. Jiao, N. L. R. Spong, O. D. W. Hughes, C. So, T. Ilieva, K. J. Weatherill, and C. S. Adams, "Single-photon stored-light Ramsey interferometry using Rydberg polaritons," *Opt. Lett.* **45**(20), 5888 (2020).
20. J. E. Palmer and S. D. Hogan, "Electric Rydberg-Atom Interferometry," *Phys. Rev. Lett.* **122**(25), 250404 (2019).
21. Q. Bouton, J. Nettersheim, D. Adam, F. Schmidt, D. Mayer, T. Lausch, E. Tiemann, and A. Widera, "Single-Atom Quantum Probes for Ultracold Gases Boosted by Nonequilibrium Spin Dynamics," *Phys. Rev. X* **10**(1), 011018 (2020).
22. A. Facon, E.-K. Dietsche, D. Grosso, S. Haroche, J.-M. Raimond, M. Brune, and S. Gleyzes, "A sensitive electrometer based on a Rydberg atom in a Schrödinger-cat state," *Nature* **535**(7611), 262–265 (2016).
23. L. A. Correa, M. Mehboudi, G. Adesso, and A. Sanpera, "Individual Quantum Probes for Optimal Thermometry," *Phys. Rev. Lett.* **114**(22), 220405 (2015).
24. N. L. R. Spong, Y. Jiao, O. D. W. Hughes, K. J. Weatherill, I. Lesanovsky, and C. S. Adams, "Collectively Encoded Rydberg Qubit," *Phys. Rev. Lett.* **127**(6), 063604 (2021).
25. M. D. Lukin, M. Fleischhauer, R. Cote, L. M. Duan, D. Jaksch, J. I. Cirac, and P. Zoller, "Dipole blockade and quantum information processing in mesoscopic atomic ensembles," *Phys. Rev. Lett.* **87**(3), 037901 (2001).
26. O. Firstenberg, C. S. Adams, and S. Hofferberth, "Nonlinear quantum optics mediated by Rydberg interactions," *J. Phys. B: At., Mol. Opt. Phys.* **49**(15), 152003 (2016).
27. Y. O. Dudin and A. Kuzmich, "Strongly Interacting Rydberg Excitations of a Cold Atomic Gas," *Science* **336**(6083), 887–889 (2012).
28. H. Busche, P. Huillery, S. W. Ball, T. Ilieva, M. P. A. Jones, and C. S. Adams, "Contactless nonlinear optics mediated by long-range Rydberg interactions," *Nat. Phys.* **13**(7), 655–658 (2017).